**Aalborg Universitet**

# Distributed Control of Battery Energy Storage Systems for Voltage Regulation in Distribution Networks with High PV Penetration

Zeraati, Mehdi ; Golshan, Mohamad Esmaeil Hamedani ; Guerrero, Josep M.

# Distributed Control of Battery Energy Storage Systems for Voltage Regulation in Distribution Networks with High PV Penetration

Mehdi Zeraati, *Student Member, IEEE,* Mohamad Esmaeil Hamedani Golshan, and Josep M. Guerrero, *Fellow, IEEE*

*Abstract*—The voltage rise problem in low voltage (LV) distribution networks with high penetration of photovoltaic (PV) resources is one of the most important challenges in the development of these renewable resources since it may prevent the maximum PV penetration considering the reliability and security issues of distribution networks. In this paper, the battery energy storage (BES) systems are used in order to solve the voltage rise during the peak PV generation as well as the voltage drop while meeting the peak load. A coordinated control strategy is proposed to regulate the charge/discharge of BESs using a combination of the local droop based control method and a distributed control scheme which ensures the voltages of feeder remain within allowed limits. Therefore, two different consensus algorithms are used: The first algorithm determines the BESs participation in voltage regulation in terms of their installed capacity whereas the second one modifies the BESs performance in terms of their state of charge (SoC) to prevent the excessive saturation or depletion of batteries. The proposed controller enables the effective use of storage capacity in different conditions. Finally, the simulation results based upon real data of a radial distribution feeder validate the effectiveness of this approach.

*Index Terms*—BES, Consensus Algorithm, Coordinated Control, LV Distribution Network, PV.

## I. INTRODUCTION

THE worldwide market for solar photovoltaic (PV) systems has been increased significantly in recent decade. The global total installed PV capacity estimated at roughly 177 GW at the end of 2014, 40 GW of which has been installed in 2014 [1]. PV has several technical and environmental advantages including power losses and congestion reduction and low carbon. The growing use of residential rooftop PVs connected to the low voltage (LV) distribution networks creates some problems such as power quality issues [2]. One of the main challenges of increasing photovoltaic resources is the voltage rise problem due to reverse power flow in distribution networks [3]. Variable generation of PV resources because of stochastic sun radiation, on the one hand, and the mismatch between generation and load peaks in most of the networks, on the other hand, can cause reverse power flow during high PV generation and low load conditions.

M. Zeraati and M. E. Hamedani Golshan are with the Department of Electrical and Computer Engineering, Isfahan University of Technology, Isfahan, 84156-83111, Iran (e-mail: m.zeraati@ec.iut.ac.ir; hgolshan@cc.iut.ac.ir).

J. M. Guerrero is with the Deepartment of Energy Technology, Aalborg University, 9220 Aalborg East Denmark (Tel: +45 2037 8262; Fax: +45 9815 1411; e-mail: joz@et.aau.dk).

Various solutions have been proposed to deal with this undesirable effect on the increase of the PV penetration in distribution networks. The simplest way is grid reinforcement. Although this solution is effective and reduces the losses in feeder, it is very expensive [4]. Another way is using the on-load tap changing (OLTC) transformers to regulate voltage at the secondary winding of distribution transformer. However, this method requires the tap to change continuously which increases tension on transformer [5].

Different control strategies have been proposed to prevent the overvoltage using reactive power control [6], [7]. Reactive power absorption by the PV inverters may put more stress on them and reduce their lifetime [8]. Moreover, it requires higher current flow on distribution feeders that results in additional losses. This solution may also reduce power factor at the sending end of feeder, depending on the reactive power absorbed by PVs. Another method is PV generation power curtailment during the overvoltage periods [9]. Due to the high R/X ratio in the LV distribution networks, the PV curtailment is more effective in comparison with the reactive power control. However, the power curtailment technique adversely affects on PV owner revenues and leads to the reduced use of the PV generation capacity [10].

The use of battery storage at the PV systems, to enable the energy storage and increase the local consumption during the peak generation periods, is an appropriate solution for replacing the power curtailment method [11], [12]. Decreasing battery cost along with technology development has made the implementation of this method reasonable. The battery can be also utilized for peak power shaving and backup power. Moreover, smoothing the PV output changes, voltage drop compensation and scheduled trading with the network can be realized using the PV storage system [13].

Different control strategies being used to control the storage systems are divided into three categories: centralized, local and distributed. A centralized method for the coordination of battery energy storage (BES) systems has been proposed in [14] to solve overvoltage problem. Authors in [15] have proposed a centralized control method for a coordinated operation of the energy storage systems and OLTC transformers for overvoltage mitigation. The centralized control methods are very effective but their performance and reliability depend on costly fast communication links [16].

The second category is the local control methods in which control commands are calculated only using locally measured

information. A coordinated control of PV and BES system has been presented in [13] for voltage control of residential distribution networks. The proposed method uses a local droop based control of BES placed at each house and does not require a complex communication infrastructure. In [12] several local voltage control strategies have been introduced using PV storage systems. These methods have robust performance, but the capability of all system resources may not be used to improve their performance [17] due to the lack of coordination between units. A charging/discharging control strategy has been developed in [18] considering the current state of charge (SoC) of the storage systems. An intelligent charging/discharging control strategy is discussed in [19] to make effective use of the storage capacity for the mitigation of voltage rise/drop problems. However, SoCs coordination is not considered in [18], [19] while the initial SoC of some batteries could be different due to the technical problems or their temporary outages.

In the third category, the distributed control strategies employ limited communication links for sharing data among different units. Distributed control methods have been applied for BESs in different applications [16], [20]–[26]. In [16], a coordinated control method composed of both local and distributed controls has been proposed for distributed BESs. In this work, an identical capacity is assumed for batteries and a similar reference waveform is considered to control the SoC of all batteries during daily operation. An energy storage management system has been developed in [20] to provide SoC balancing in dc microgrids. Dynamic energy level balancing between BESs has been developed in [21] to improve frequency regulation in islanded microgrids. The proposed strategy is designed based on cooperative state variable feedback control, assuming each agent has access to its states, and the full states of its neighbors. This requires massive data communications between BES units. In [22], a cooperative control strategy has been employed to coordinate power sharing between heterogeneous energy storage devices with batteries and ultracapacitors. A distributed control strategy has been presented in [23] for SoC balancing between the battery modules of a reconfigurable BES system. A balanced charging/discharging strategy has been developed in [24] that shares charge/discharge currents between interconnected heterogeneous battery systems to maintain uniform SoCs during the operation. However, SoC balancing is done in [23], [24] for the battries in a single BES and the calculation method of the power to be exchanged is not discussed. A distributed algorithm has been presented in [25] to regulate output power of dispersed energy storage systems (DESSs). The algorithm satisfies both the fair utilization among the DESSs and the power balance of power system. The main objectives of implemented consensus algorithm in [26] are minimizing the total power losses associated with charging/discharging inefficiency of energy storage systems and maintaining the supply-demand balance in an islanded microgrid. [25], [26] do not consider the technical limitations of energy storage systems such as capacity and SoC, while these parameters may have major impacts on energy storage system operation and lifetime.

In this paper, a control strategy is proposed for BESs used in the rooftop PV systems to mitigate the voltage rise/drop problems in the LV distribution networks with high penetration of PV sources. Technical limitations of energy storage systems such as capacity and SoC are simultaneously considered along with the voltage control. The proposed control scheme includes a local droop based control method and a distributed control algorithm. The local droop algorithm determines the charge/discharge starting instant and the initial power to be exchanged by BESs at each bus. The distributed control is employed to coordinate the BESs that generally have different capacities and unequal initial SoCs. The coordinated control is based on two consensus algorithms, the weighted consensus control (WCC) algorithm and the dynamic consensus control (DCC) algorithm. The combination of these algorithms leads to efficient utilization of BESs capability to regulate voltage. The WCC algorithm determines the storages participation in voltage regulation in a fair way proportional to their capacity. The DCC algorithm modifies storages participation in order to prevent early and excessive saturation or depletion considering the SoC of BESs.

The paper is organized as follows. The theory of voltage deviations in the distribution feeders with high penetration of PV cells is explained in section II. The proposed control strategy is presented in section III. Section IV introduces the test distribution system and presents simulation results. Finally, Section V concludes the paper.

## II. PROBLEM DESCRIPTION

Using BES in the residential rooftop PV systems is one of the effective methods for solving both problems in the distribution networks with high penetration of PV resources, the voltage rise and the voltage drop under the peak PV generation and the peak load periods, respectively. In this section, a simple radial feeder is used to describe the voltage rise/drop problems.

### A. Voltage Rise/Drop in a Radial Distribution feeder

Figure 1(a) shows a simple radial distribution feeder. Bus 2 includes a PV panel, a BES and a local residential load. Figure 1(b) illustrates the equivalent circuit of the feeder. In the circuit analysis, the effect of the BES is ignored temporarily. In this diagram, the net power injection of the PV and the load connected to the point of common coupling (PCC) is considered as a current source. $\overline{V}_n = |\overline{V}_n|\underline{/0°}$ is the PCC voltage. $\overline{Z}$ is the impedance from the PCC to the MV/LV distribution transformer located at the beginning of the feeder. $\overline{V}_G$ is the constant voltage of bus 1. The voltage deviation $\Delta\overline{V}$ along the feeder, due to the current injection $\overline{I}_n$ at bus n, can be expressed as

$$\Delta\overline{V} = \overline{Z}.\overline{I}_n \tag{1}$$

where $\overline{I}_n$ is calculated by the complex power at bus n, $\overline{S}_n$ (comprised of real power $P_n$ and reactive power $Q_n$) as

$$\overline{I}_n = (\frac{\overline{S}_n}{\overline{V}_n})^* = (\frac{P_n}{\overline{V}_n} - j\frac{Q_n}{\overline{V}_n}) \tag{2}$$
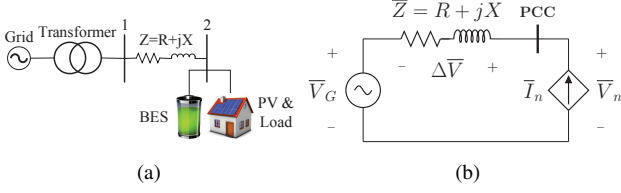
Fig. 1: The distribution feeder. (a) A typical bus with PV and BES systems; (b) The equivalent circuit.



Fig. 2: Voltage profiles along the radial distribution feeder. (a) Voltage rise; (b) Voltage drop.

Expressing the feeder impedance in terms of its resistance R and its reactance X and substituting (2) in (1), $\Delta\overline{V}$ can be written as

$$\Delta\overline{V} = \frac{R.P_n + X.Q_n}{|\overline{V}_n|} + j\frac{X.P_n - R.Q_n}{|\overline{V}_n|} \quad (3)$$

The voltage deviation, $\Delta\overline{V}$, has a component $\Delta V_d$, along the axis of the phasor $\overline{V}_n$, and a component $\Delta V_q$, 90 degree out of phase with $\overline{V}_n$:

$$\Delta V_d \triangleq \frac{R.P_n + X.Q_n}{|\overline{V}_n|} \quad (4)$$

$$\Delta V_q \triangleq \frac{X.P_n - R.Q_n}{|\overline{V}_n|} \quad (5)$$

Therefore, the magnitude of $\overline{V}_G$ can be expressed as

$$|\overline{V}_G| = [(|\overline{V}_n| - \Delta V_d)^2 + (\Delta V_q)^2]^{1/2} \quad (6)$$

Since $\Delta V_q$ is very smaller than $(|\overline{V}_n| - \Delta V_d)$, $|\overline{V}_n|$ can be approximately written as

$$|\overline{V}_n| = |\overline{V}_G| + \Delta V_d \quad (7)$$

On the other hand, the component $\Delta V_d$ can be approximated by substituting $|\overline{V}_n|$ by $|\overline{V}_G|$.

$$\Delta V_d \approx \frac{R.P_n + X.Q_n}{|\overline{V}_G|} \quad (8)$$

Finally, we obtain

$$|\overline{V}_n| \simeq |\overline{V}_G| + \frac{R.P_n + X.Q_n}{|\overline{V}_G|} \quad (9)$$

Given that $R/X$ ratio is usually high in the LV distribution networks, the net real power, $P_n$, considerably affects the PCC voltage magnitude, $|\overline{V}_n|$.

One can assume the reactive power control is not used in PV control scheme, and the $Q_n$ value related to load is constant in (9). If the net real power injected by the PV and the load ($P_n$) to the PCC is positive (i.e., generation is greater than load), the voltage can increase along the feeder. On the other hand, if $P_n$ is negative (i.e., load is greater than generation), the voltage decreases along the feeder.

Figure 2 shows the typical voltage profiles along a radial distribution feeder. Figures 2(a) and 2(b) illustrate the voltage rise in PV peak generation period and the voltage drop in peak load period, respectively. Depending on the power flow and its direction, voltages along the feeder may increase or decrease. According to the existing standards, for connecting the inverter-based distributed generation resources to the LV
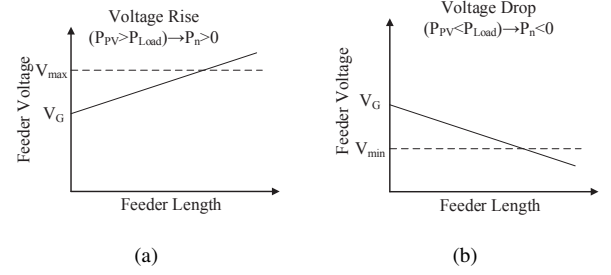
distribution networks, various voltage limits are considered for operation in normal and critical conditions [3]. Although the networks are allowed to be operated up to the critical voltages, but if the voltage at each point of the system violates the minimum or maximum thresholds, some corrective actions should be taken to improve network voltage profile. According to IEEE standard 1547, the maximum and minimum critical voltages are 1.1 p.u. and 0.88 p.u., respectively. Violation of these voltages necessitates disconnection of the distributed generations (DGs) from the network [27]. The thresholds of starting corrective actions should be lower than the critical voltages. For example, it is possible to select the allowed voltage deviations equal to ±0.05 p.u.

By adding the BES to PVs, a DG unit with dispatchable output is obtained which can be controlled according to desired aims. In this way, charging and discharging of the BESs respectively in peak generation and peak load conditions, decrease the difference between PV generation and load demand and the voltage rise/drop problems could be eliminated.

## III. PROPOSED COORDINATED CONTROL STRATEGY

Figure 3 shows the block diagram of the proposed control strategy for the PV system located at the $n$th bus, where solid and dotted lines show power flow and control signals, respectively. The PV panel is connected to the DC link of the inverter through a boost converter which regulates the DC link voltage. A bidirectional converter connects the BES system to the inverter for enabling power exchange. The PV control is based on maximum power point tracking (MPPT). Power injection by MPPT algorithm might cause overvoltage in distribution feeders in the period of PV peak generation.

Real power injection from PV inverter can be limited by storing the extra power in the BES system. In this way, the voltage rise problem will be alleviated. Moreover, in peak load periods which usually coincide with low PV generation, the stored energy in batteries can be used for voltage drop compensation at the ending buses of the feeder.

In this section, a new method for charge/discharge coordination of batteries is presented. The proposed method is a combination of local droop based control and distributed consensus control algorithms each of which has been used for specific objectives. If the voltage at any bus deviates from the pre-defined limits, the local droop based control determines the initial exchanged (charge/discharge) power for the BES.
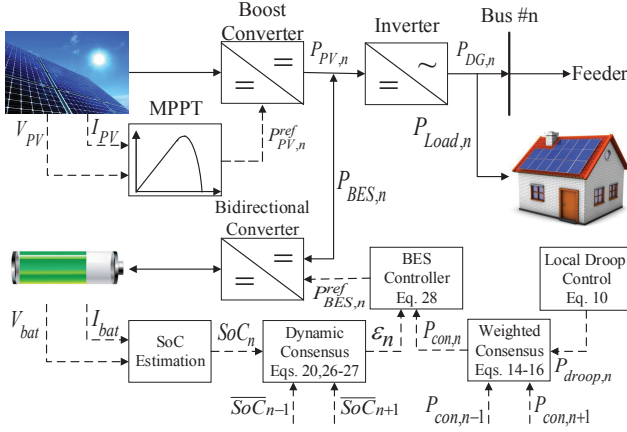
Fig. 3: The block diagram of the proposed control strategy for the $n$th bus.

Then, based on data communication between units through limited communication links, the coordinated voltage control strategy determines how BESs participate in voltage profile improvement. To this aim, the WCC algorithm shares the total required power among batteries proportional to their capacities. Simultaneously, the DCC algorithm adjusts the output power of BESs based on their SoC to prevent batteries from early saturation and depletion and enable the effective use of available capacity of storage systems.

### A. Local Droop Based Control

In the proposed control method, an initial power value is calculated at each bus to be exchanged in voltage rise/drop conditions. A droop control method determines the amount of exchanged power between the BES and the network based on a droop function when the voltage deviation violates the allowed limits. Due to the fact that the minimum and maximum threshold voltages could be different, two distinct droop functions are defined for charge and discharge modes. Therefore, the initial charging/discharging power of each BES is calculated locally based on the following law

$$P_{droop,n} = \begin{cases} m_d(V_n - V_{thr_d}) & V_n < V_{thr_d} \\ 0 & V_{thr_d} \leq V_n \leq V_{thr_c} \\ m_c(V_n - V_{thr_c}) & V_n > V_{thr_c} \end{cases} \quad (10)$$

During the period of peak PV generation, if the voltage amplitude at the $n$th bus ($V_n$) exceeds the charge threshold voltage $V_{thr_c}$, $P_{droop,n}$ will be positive that means BES absorbs power. During the period of peak load, if $V_n$ is less than the discharge threshold voltage $V_{thr_d}$, $P_{droop,n}$ will be negative that means BES injects power into the network. Otherwise, $P_{droop,n}$ will be zero that indicates storage systems do not participate in voltage control.

Droop coefficient in charge mode ($m_c$) is calculated as a function of the maximum load ($P_{L,max}$) and the PV maximum generation ($P_{PV,max}$):

$$m_c = \frac{P_{PV,max} - P_{L,max}}{V_{thr_c} - V_{nom}} \quad (11)$$

where $V_{nom}$ is the distribution network nominal voltage. The portion of $n$th PV power which is going to be stored in the battery during overvoltage period is calculated based on $m_c$. According to the droop method, BES starts to charge when the voltage at the relevant bus is greater than $V_{thr_c}$.

Conversely, when the voltage at the $n$th bus is less than $V_{thr_d}$, the BES starts to inject power into the network. The amount of injected power is calculated using $m_d$, the droop coefficient in discharge mode, which is determined as

$$m_d = \frac{P_{PV,max} - P_{L,max}}{V_{nom} - V_{thr_d}} \quad (12)$$

Coefficients $m_c$ and $m_d$ are defined by five parameters: $P_{PV,max}$, $P_{L,max}$, $V_{thr_c}$, $V_{thr_d}$ and $V_{nom}$. The larger difference of peak PV generation and peak load leads to larger $m_c$ or $m_d$. This means that the BES participate more in the voltage regulation. The similar effect can be achieved by smaller $V_{thr_c} - V_{nom}$ or $V_{nom} - V_{thr_d}$.

If only the droop based control according to (10) is used, the BESs located at the end of the feeder may participate more in the voltage regulation in comparison with other BESs. Because, in many cases, only a few buses at the end of the feeder experience voltage violation from pre-defined limits. As a result, some energy storage systems do not sense voltage rise/drop and therefore, are not activated for voltage control.

In addition, some BESs might be fully charged/discharged during the voltage regulation process due to different capacity or initial SoC and unpredictable weather and load conditions. Thus, correcting the voltage control is necessary for fair participation of BESs to maximize the utilization of available batteries capacity in the network. To this aim, a distributed control strategy using consensus algorithms is added to BESs controller to effectively employ their available storage capacity. The consensus algorithms are executed by sharing necessary data among all existing units. The proposed distributed control strategy works based on data communication including output power and SoC between neighbor units in order to adjust the charging/discharging rate of BESs.

### B. Participation of Storage Systems Proportional to Their Installed Capacity: WCC Algorithm

It is important for all the BESs in a distribution network to be controlled in a fair way for participating in the voltage regulation process. Using limited communication links among BESs and without a central controller, the WCC algorithm proposed in [28] is adopted to achieve a distributed control for fair charging/discharging of BESs. WCC is a distributed control strategy that can be used to coordinate all subsystems.

As explained in subsection III.A, when voltage rise/drop is detected in the network, $P_{droop,n}$ is calculated at each bus, by droop function (10) at defined intervals, and it is used as starting point of the WCC algorithm. Then, the coordination of units is realized by the WCC algorithm.

Assume that the controlled network has $r$ BESs. Buses with BES are linked together by a communication network. As seen in Fig. 4, the established communication network for creating links among BESs can be expressed with a directed graph $G(V,E)$, where $V = \{v_1, ..., v_r\}$ is set of nodes and
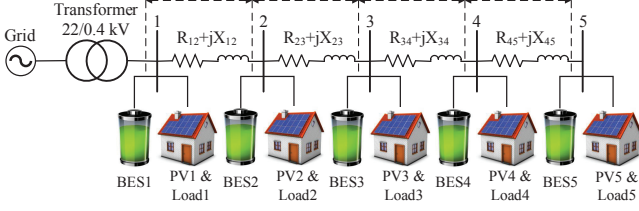
Fig. 4: The distribution feeder with PV and BES systems and communication network.

$E \subseteq V \times V$ is set of edges. The element $(v_n, v_m)$ (directed edge from node $v_n$ to node $v_m$) indicates a link between bus $v_n$ and $v_m$. Hence, $(v_n, v_m) \in E$ means possibility of data communication from bus $v_n$ to bus $v_m$. Total number of communication links in $E$ is denoted by $l_s$. For example, the system shown in Fig. 4 has 5 storage systems where each one only receives the information from the neighbors. The associated adjacency matrix $A = [a_{nm}] \in \Re^{r \times r}$ contains weighting coefficients, where $a_{nm} > 0$ if $(v_n, v_m) \in E$ and $a_{nm} = 0$, otherwise. The set of all neighbors of node n is denoted by $N_n = \{m \mid (v_n, v_m) \in E\}$. The in-degree and out-degree matrices $D^{in} = diag\{d_n^{in}\}$ and $D^{out} = diag\{d_n^{out}\}$ are diagonal matrices with $d_n^{in} = \sum_{m \in N_n} a_{nm}$ and $d_n^{out} = \sum_{n \in N_m} a_{mn}$, respectively. The Laplacian matrix is defined as $L \triangleq D^{in} - A$ which is balanced if $D^{in} = D^{out}$.

At time $t$, bus $n$ has a controllable power $P_{con,n}^t$, injected into or absorbed from the network by BES. A weight, $\mu_n$, is assigned to $P_{con,n}$ at bus $n$, which its value is selected considering the control goal. The goal of the distributed control for BESs, in this paper, is to achieve a consensus on their exchanged weighted power, i.e., $P_{con,n}/\mu_n \rightarrow \eta \; n = 1, ..., r$, where $\eta$ is a constant. In the proposed control, $\mu_n$ is selected equal to the capacity of $BES_n$. Thus, the storage systems participate in voltage regulation proportional to their capacity.

Consider state vector $P_{con}^t = [P_{con,1}^t, ..., P_{con,n}^t, ..., P_{con,r}^t]$ which indicates the exchanged power of BESs in control step $t$, weighting coefficients vector $\mu = [\mu_1, ..., \mu_n, ..., \mu_r]$ and state scaling matrix $\gamma = diag[1/\mu_1, ..., 1/\mu_n, ..., 1/\mu_r]$. If $I$ shows a column vector which all of its elements are 1, the goal of WCC is $\gamma P_{con}^t = \eta I$, where $\eta = \sum_{n=1}^r P_{con,n}/(\mu_1 + ... + \mu_r)$. The most important characteristic of this control strategy is that for all $t$:

$$\sum_{n=1}^r P_{con,n}^1 = \cdots = \sum_{n=1}^r P_{con,n}^t = \cdots = \sum_{n=1}^r P_{con,n} \quad (13)$$

This means that, total exchanged power of storage systems with the network in all the time steps of running the algorithm is the same as the total initial values in starting instant. Although none of BESs has the system information completely, a global coordination is achieved for all states through implementing suitable rules. These rules control BESs using both the local and neighbors information, including $P_{con}^t$ and $\mu$.

For a specified period $T$, the consensus algorithm is run in discrete steps $tT, t = 1, 2, ...$ in order to update the exchanged

power of BESs. In each control step, the exchanged power is updated from $P_{con}^t$ to $P_{con}^{t+1}$ using $u^t$ as

$$P_{con,n}^{t+1} = P_{con,n}^t + u_n^t \quad (14)$$

Now the main problem is determining $u_n^t$ in each discrete control step. To this aim, it is assumed that each BES has a link with its neighbors. Two BESs are considered neighbor when there is at least one communication link between them. Then, $u_n^t$ can be calculated using the control signal, $\lambda_{nm}^t$, considering the information from the neighbor units:

$$u_n^t = \sum_{(v_n, v_m) \in E} \lambda_{nm}^t + \sum_{(v_m, v_n) \in E} \lambda_{mn}^t \quad (15)$$

The control signal $\lambda_{nm}^t$, is defined by (16) which reflects the weighted difference between exchanged power of BESs located at both sides of the communication link $(v_n, v_m)$:

$$\lambda_{nm}^t = \frac{P_{con,n}^t}{\mu_n} - \frac{P_{con,m}^t}{\mu_m} \quad (16)$$

where $\mu_n$ and $\mu_m$ are weighting coefficients that can be selected from BESs characteristics at bus $n$ and $m$, respectively. As mentioned before, weighting coefficients are selected according to installed capacity of batteries.

To better presentation of the above process, (14)-(16) can be rewritten in the following matrix form:

$$\lambda^t = H_2 \gamma P_{con}^t - \hat{\gamma} H_1 P_{con}^t = H P_{con}^t \quad (17)$$

$$u^t = -(H_2 - H_1)^T H P_{con}^t \quad (18)$$

where $H_1$ is a $l_s \times r$ matrix, $r$ is the total number of buses with installed BES and $l_s$ is the total number of communication links. If the communication link $(v_n, v_m)$ is the $l$th link in $E$, then all the elements of $l$th row in $H_1$ are zero except the $m$th element which is 1. $H_2$ is a $l_s \times r$ matrix. If the communication link $(v_n, v_m)$ is the $l$th link in $E$, then all the elements of $l$th row in $H_2$ are zero except the $n$th element which is 1. $\gamma$ is a $r \times r$ diagonal matrix whose $n$th diagonal element is $1/\mu_n$. $\hat{\gamma}$ is a $l_s \times l_s$ diagonal matrix whose $l$th diagonal element is $1/\mu_m$, if the $l$th link in the $E$ set is $(v_n, v_m)$.

Assuming $I$ and $0$ represent two $l_s$-dimensional column vector with all 1 and 0 elements, respectively, it can be proved that $\hat{\gamma} H_1 \gamma^{-1} = H_1$, $H \gamma^{-1} I = (H_2 - H_1) I = 0$ and $\gamma^{-1} I = \mu$. As a result

$$I^T u^t = I^T (H_2 - H_1)^T H P_{con}^t = 0 \quad (19)$$

The sum of updated values always equals zero. Therefore, according to (13), this strategy assures that the total amount of exchanged power at each updating step remains unchanged in WCC algorithm.

The WCC algorithm shares the total initial powers calculated by the droop control proportional to BESs capacity. Since this algorithm does not consider the energy level of BESs, it is expected that the batteries with higher initial SoC will become full in the charge mode. Once a BES becomes full, it can not contribute to decrease the voltage rise during periods of high PV generation. In addition, the remained BESs may not be able to provide the required power for voltage regulation. Similarly, if a battery runs out of energy then it can no longer inject

power during periods of peak load, which leads to degrading the voltage regulation process.

In order to prevent BESs from early running out of service, the capacity based control strategy can be modified so that the BESs contribute in voltage regulation considering their energy level. On the other hand, in the case that BESs control is only based on their SoC, when the power absorption by some batteries decrease due to running full of energy, the capacity of other BESs with lower SoC may be less than the required power for voltage control. Hence, the combined control strategy consists of both WCC and DCC algorithms is proposed.

Therefore, droop based control determines the total required power for voltage regulation. This power is shared among BESs by WCC proportional to their capacities. Then the WCC algorithm is cooperated with the DCC algorithm to avoid early saturation/depletion of BESs. The combined control scheme presents improved performance with respect to only considering droop control, BESs capacity or BESs SoC.

### C. Participation of Storage Systems Proportional to Their SoC: DCC Algorithm

The explained strategy in subsection III.B is based on the capacity of BESs without considering the SoC of batteries. However, the BESs might have unequal initial SoC because of the uneven charge/discharge during operation and battery disconnection due to the cloud passing effect or technical problems. As a result, the participation capability of a battery in voltage control would be decreased due to its excessive charge/discharge. In this subsection, a DCC algorithm based on storage systems SoC is presented to keep the energy level of BESs close together as far as possible. The main idea of this algorithm is based on the average SoC estimation of all batteries in a distributed manner and calculating a correction factor to modify their participation in voltage profile improvement process. The correction factor is calculated by comparing the SoC of each battery and the estimated average SoC across the network.

Equation (20) shows an designed observer to estimate the system average SoC based on a DCC framework. The observer at bus $n$ receives the neighbor estimations and then updates its estimation ($\overline{SoC}_n$) as

$$\overline{SoC}_n = SoC_n + \int_0^\tau \sum_{m \in N_n} a_{nm}(\overline{SoC}_m - \overline{SoC}_n)d\tau \quad (20)$$

This updating protocol is known as DCC algorithm [29]. It has been proved that this local averaging converges to an consensus value which is the true average SoC [30].

According to (20), any SoC variation of each BES, would immediately affect the $\overline{SoC}$ estimation of BES. The variation in $\overline{SoC}$ would propagate across the network and affect all other estimations. By differentiating (20), we have

$$\dot{\overline{SoC}}_n = \dot{SoC}_n + \sum_{m \in N_n} a_{nm}(\overline{SoC}_m - \overline{SoC}_n)$$
$$= \dot{SoC}_n + \sum_{m \in N_n} a_{nm}\overline{SoC}_m - d_n^{in}\overline{SoC}_n \quad (21)$$

Then, the global averaging dynamic can be formulated as

$$\dot{\overline{SoC}} = \dot{SoC} + A\overline{SoC} - D^{in}\overline{SoC} =$$
$$\dot{SoC} - (D^{in} - A)\overline{SoC} = \dot{SoC} - L\overline{SoC} \quad (22)$$

where $SoC = [SoC_1, ..., SoC_r]^T$ and $\overline{SoC} = [\overline{SoC}_1, ..., \overline{SoC}_r]^T$ are the measured SoC and the estimated average SoC vectors, respectively. Eq. (23) is obtained by applying Laplace transform to Eq. (22).

$$s\overline{SOC} - \overline{SOC}(0) = sSOC - SOC(0) - L\overline{SOC} \quad (23)$$

where $SOC$ and $\overline{SOC}$ are the Laplace transforms of $SoC$ and $\overline{SoC}$, respectively. Since $\overline{SOC}(0) = SOC(0)$ according to (20), therefore we obtain

$$\overline{SOC} = s(sI_r + L)^{-1}SOC = H_{ave}SOC \quad (24)$$

where $I_r \in \Re^{r \times r}$ and $H_{ave}$ are the identity matrix and the averaging transfer function, respectively. It is shown in [30] that if $L$ is balanced, all estimations converge to a global consensus, which is the true average of the SoC values across the network.

$$\lim_{t \to \infty} \overline{SoC}_n = \frac{1}{r} \sum_{n=1}^{r} SoC_n(t) \quad (25)$$

Then, the control rules in (26) and (27) are defined to calculate the participation correction factor (PCF) of batteries in charge ($\varepsilon_{n,c}$) and discharge ($\varepsilon_{n,d}$) modes, respectively, in order to maintain uniform their SoC:

$$\varepsilon_{n,c} = \begin{cases} 0 & SoC_n > SoC_{max} \\ 1 - k \times \left(\frac{SoC_n - \overline{SoC}_n}{100}\right) & SoC_n \leq SoC_{max} \end{cases} \quad (26)$$

$$\varepsilon_{n,d} = \begin{cases} 1 + k \times \left(\frac{SoC_n - \overline{SoC}_n}{100}\right) & SoC_n \geq SoC_{min} \\ 0 & SoC_n < SoC_{min} \end{cases} \quad (27)$$

where $k$ is a constant used to speed up the convergence. To more explanation of the control logic, consider (26) to calculate the $\varepsilon_{n,c}$. If a battery SoC in real time ($SoC_n$) is greater than the estimated average SoC ($\overline{SoC}_n$), then $\varepsilon_{n,c} < 1$. This means that $P_{con,n}$, determined using WCC algorithm, should be decreased. Conversely, if $SoC_n < \overline{SoC}_n$, then $\varepsilon_{n,c} > 1$ and $P_{con,n}$ should be increased. It should be noted that if a battery SoC reaches its maximum allowed saturation ($SoC_{max}$), the BES will be removed from the voltage regulation process. The same reasoning can also be used for discharge mode. If $SoC_n > \overline{SoC}_n$, then the BES participation in voltage profile improvement should be increased, and vice versa. As before, the BES will be disconnected when the SoC of the battery reaches to its minimum allowed depletion ($SoC_{min}$).

In subsection III.B, the BES exchanged power ($P_{con,n}$) calculated such that the charge/discharge power to storage capacity ratio is identical for all BESs. When batteries have different SoC, this strategy may cause early saturation or depletion in some units. To avoid this problem, the $\varepsilon_n$ is applied to modify the BESs participation. In charge/discharge mode, it is desirable that the storage systems with smaller/larger SoC have higher participation in voltage rise/drop mitigation until the SoC of all BESs move to an identical value gradually.

TABLE I: Cable Data for the Studied Feeder

| No of conductors and cross sectional area ($mm^2$) | Maximal resistance of conductor at $20°$ ($\Omega$/km) | Reactance of conductor ($\Omega$/km) |
|---|---|---|
| 1×95 | 0.3211 | 0.0892 |
| 4×95 | 0.3211 | 0.0691 |
| 4×120 | 0.2539 | 0.0691 |
| 4×150 | 0.2060 | 0.0691 |

Thus, the exchanged power of the BES at bus $n$ is determined as

$$P_{BES,n}^{ref} = \varepsilon_n \times P_{con,n} \tag{28}$$

where $P_{BES,n}^{ref}$ is the charging/discharging active power of the $n$th BES. However, there are charging/discharging losses due to the battery internal resistance. This is modeled by introducing charging/discharging efficiencies as

$$P_{BES,n}^{ref,c} = \eta_n^c P_{BES,n}^{ref} \tag{29}$$

$$P_{BES,n}^{ref,d} = P_{BES,n}^{ref}/\eta_n^d \tag{30}$$

where $P_{BES,n}^{ref,c}$ and $P_{BES,n}^{ref,d}$ are the actual power absorbed and injected by the $n$th BES, respectively, and $\eta_n^c$ and $\eta_n^d$ are the corresponding charging and discharging efficiencies.

Depending on the type of study, $\eta_n^c$ and $\eta_n^d$ can be approximated by one [20], [23], similar constant values [31], different constant values [32], and as functions of the charging/discharging rate of BESs [26]. It has been shown in [33] based on experiments that the charging efficiency has a linear relationship with the charging rate as

$$\eta_n^c = \alpha_n - \beta_n P_{BES,n}^{ref} \tag{31}$$

where $\alpha_n$ , $\beta_n$ are constant coefficients for $n$th BES. The discharging mode can be dealt with in the same way.

## IV. APPLICATION OF THE PROPOSED CONTROL SCHEME TO A TEST NETWORK

### A. Network Data and Description

In this section, a realistic 7-bus LV radial feeder [11] shown in Fig. 5 is modeled in Matlab/Simulink to assess the performance of the proposed control strategy. This residential feeder supplies 33 customers through a 185 KVA, 22/0.4 kV transformer. It is composed of NA2XRY type LV cables with parameters given in Table I. As seen, the average R/X ratio of cables is about 4.1. The system includes 9 rooftop PVs which are operated in unity power factor. According to presented results in [11], to prevent overvoltage situations, a maximum 6 kW/40 kWh battery is required for the PV systems. The size of each BES has been selected proportional to the PV capacity for the purposes of this study. Installed PVs capacity and BESs size are given in Fig. 5. The secondary voltage of the transformer is set at 1.0 p.u.. The maximum allowed voltage deviation along the feeder is assumed %5 which results in threshold voltages of 1.05 p.u./0.95p.u. in charge/discharge mode ($V_{thr_c}/V_{thr_d}$).

To assess the proposed methodology in a realistic condition, the profiles of PVs output and residential loads are considered
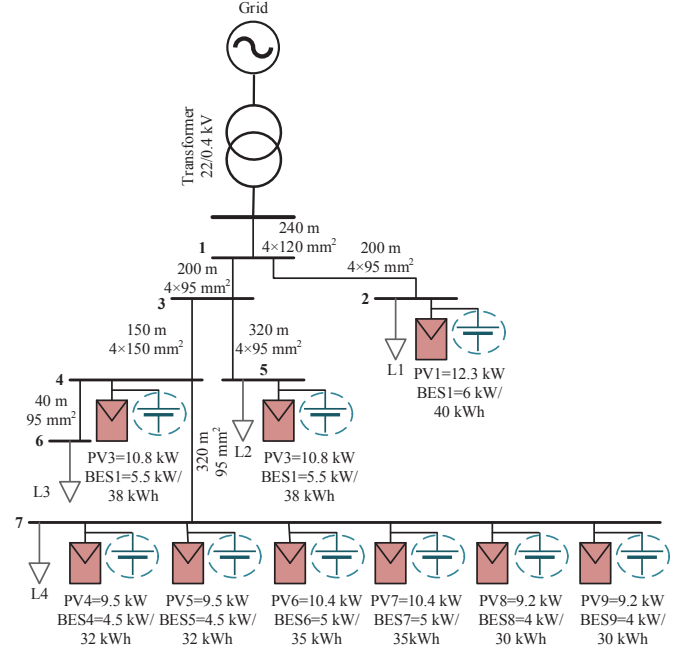


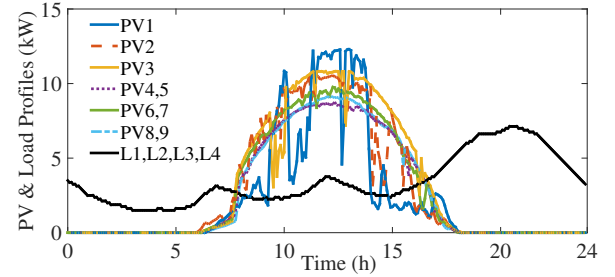Fig. 5: Single line diagram of LV radial distribution feeder.



Fig. 6: Output power profiles of different PVs and the load profile of a typical residential feeder in Isfahan.

as real data related to Isfahan, Iran. The 5-minute PV data were measured at 20 kW solar plant of Isfahan University of Technology in the winter of 2015. Then, these data were rescaled for each PV of test feeder proportional to its maximum power. Moreover, six different profiles, shown in Fig. 6, are defined for the 9 PV systems in order to model the difference between PVs output resulting from factors such as cloud passing. The feeder loads profile is assumed identical according to a residential distribution feeder in Isfahan, which is shown in Fig. 6. The parameters of the control strategy are given in Table II. The charging/discharging efficiencies of BESs are assumed 100% except for subsection IV.E.

### B. Droop Based Control

The first test case demonstrates the performance of the droop based control method without the proposed distributed control strategy. Figure 7 shows the voltage profile of the feeder buses while there is no BES and PVs are controlled in MPPT mode. The maximum voltage (1.085 p.u.) and the minimum voltage (0.906 p.u.) are experienced at bus 7, the end bus of the feeder, respectively at the midday and evening. As seen, during some

TABLE II: Parameters of Proposed Control Method

| Charging/Discharging Efficiency Coefficients | | | | |
|---|---|---|---|---|
| $\alpha_{c,d_1}$=0.79 | $\alpha_{c,d_{2,3}}$=0.83 | $\alpha_{c,d_{4,5}}$=0.88 | $\alpha_{c,d_{6,7}}$=0.92 | $\alpha_{c,d_{8,9}}$=0.85 |
| $\beta_{c,d_1}$=0.005 | $\beta_{c,d_{2,3}}$=0.006 | $\beta_{c,d_{4,5}}$=0.009 | $\beta_{c,d_{6,7}}$=0.01 | $\beta_{c,d_{8,9}}$=0.008 |
| Local Droop Based Control | | | | |
| $m_{c,d_1}$=522 | $m_{c,d_{2,3}}$=478 | $m_{c,d_{4,5}}$=391 | $m_{c,d_{6,7}}$=435 | $m_{c,d_{8,9}}$=348 |
| WCC Algorithm | | | | |
| $\mu_1$=6 | $\mu_{2,3}$=5.5 | $\mu_{4,5}$=4.5 | $\mu_{6,7}$=5 | $\mu_{8,9}$=4 |
| DCC Algorithm | | | | |
| $SoC_{min}$=20 | | $SoC_{max}$=80 | | $k$=5 |



(a)



Fig. 7: 24-hour voltage profile without BESs.


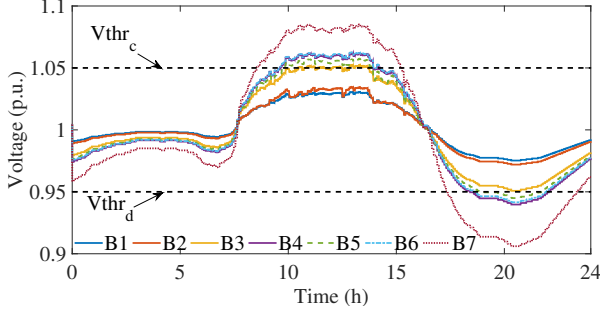
(b)

Fig. 8: Droop based control of BESs. (a) 24-hour voltage profile; (b) The SoC variations of BESs.

periods, the voltage at buses 4, 5, 6, and 7 exceed the charge threshold voltage (1.05 p.u.) and they experience overvoltage. On the other hand, during some periods, the voltage at the same buses decreases down the discharge threshold voltage (0.95 p.u.) and they experience voltage drop.

Figures 8(a) and 8(b) present the voltage and SoC profiles when the BESs are only controlled with droop based method. As seen, if only the droop based control is used, the BESs located at the end of the feeder (BESs 4-9) participate more than the other BESs in the voltage regulation. Other energy storage systems (BESs 1-3) do not sense voltage rise/drop and therefore, they are not activated for voltage control. Buses 4-7 experience overvoltage from 13:00 h to 16:00 h, because the BESs 4-9 are full of energy and they can no longer participate in voltage regulation.

### C. Coordinated Control Scheme without DCC Algorithm

The studies of this subsection demonstrate the capability of the control strategy in determining the BESs participations based on their installed capacity. The weighting coefficients $\mu_n$ given in Table II have been calculated according to the capacity of BESs depicted in Fig. 5.

In the next study, the local droop based control and WCC algorithm are implemented to control the charge/discharge of BESs coordinately. All other conditions are as the same as previous. The 24-hour profile of bus voltages are presented in Fig. 9(a). It can be seen that, using the installed BESs, the voltage is regulated to lower than charge mode threshold during overvoltage period, and to higher than discharge mode threshold during voltage drop period. Thus, the voltage rise/drop problems are mitigated completely.
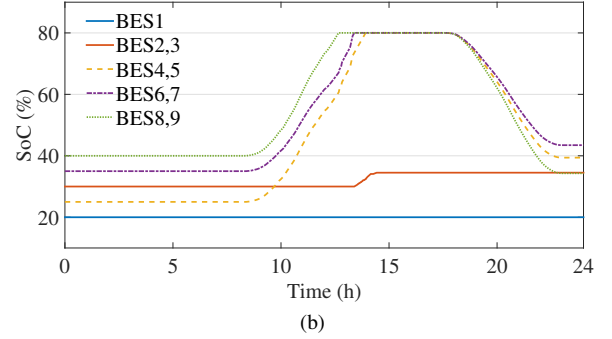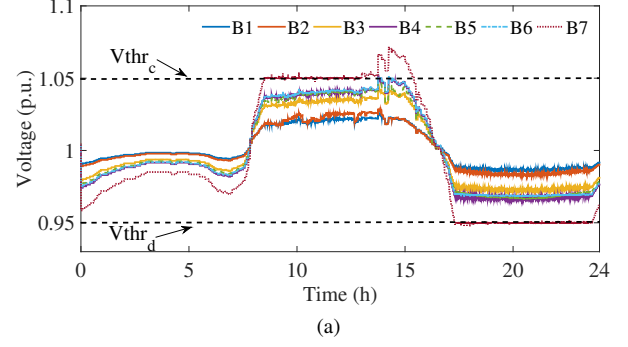
Figure 9(b) illustrates the participation percent of BESs in terms of their capacity. The main idea of the developed WCC algorithm is to achieve an identical percentage of participation for all BESs during the operation time. The larger the capacity of the installed battery, the more its participation in voltage regulation, and vice versa. The fluctuations at the beginning of intervals are due to the initial exchanged power of BESs, determined by the droop based control method which converge to a certain value after a short time.

In this case, the SoC of BESs is not considered. Hence, it does not influence their charge/discharge rate. The 24-hour variation of SoCs is shown in Fig. 10(a), considering an identical initial SoC of %30 for all BESs. Since the BESs are controlled proportional to their capacity, SoCs also change almost uniformly. In this case, for the sake of simplicity, it is assumed that BESs have not any limitation in view of full saturation or depletion for voltage regulation process and they will not reach their upper and lower SoC limits during a day. However, owing to reduction of battery lifetime [27], if a battery is not allowed to be operated out of its designed SoC limits (e.g., %20-%80), this strategy will not function properly. Figure 10(b) shows the SoC variations for different initial values. As the SoC of BES1 exceeds the maximum limit (%80), regarding to the explanations above, the control strategy has poor performance. This drawback will be resolved in the next case study using the proposed correction factor.

### D. Coordinated Control Scheme with DCC Algorithm

In this subsection, the proposed PCF ($\varepsilon_n$) is employed to coordinate the SoC of storage systems in both charge and
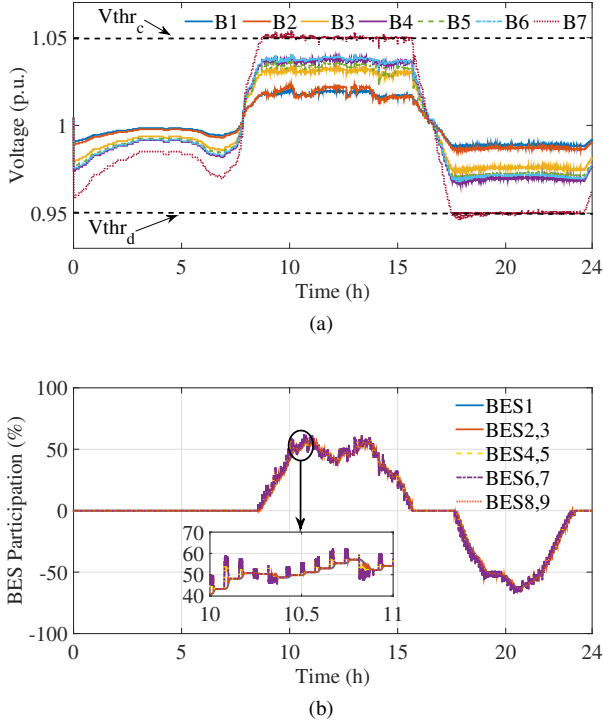
Fig. 9: Coordinated control scheme without DCC algorithm. (a) 24-hour voltage profile; (b) BES participation.
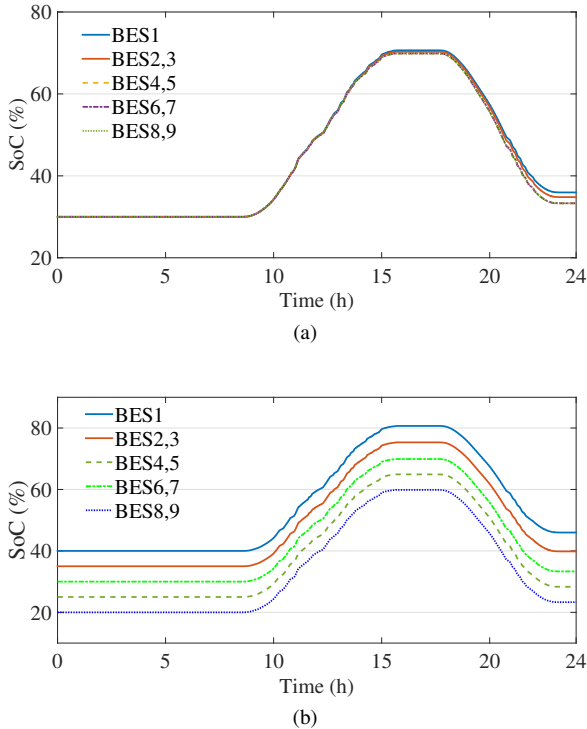


Fig. 10: The SoC variations of BESs. (a) With identical initial SoCs; (b) With different initial SoCs.

discharge modes. All simulation conditions are as the same in subsection IV.C. To provide a comparison with the previous study, the initial SoCs of BESs are set according to Fig. 10(b). In this case study, the charging/discharging rate is controlled in an attempt to prevent early saturation/depletion of storage systems. As a result, all available capacity of BESs could be employed to improve the voltage profile.

Figures 11(a) and 11(b) show the 24-hour profiles of bus voltages and the SoC of BESs, respectively. As seen in Fig. 11(a), the proposed algorithm can effectively prevent the overvoltage at midday and voltage drop at evening, and, hence the system voltage limits are not violated. In addition, although the initial SoCs are different, they gradually get closer over time and remain within allowed limits in contrast to Fig. 10(b). It should be noted that, the SoCs convergence procedure continues over time. Participation percent of BESs is shown in Fig. 11(c). At initial hours, BESs present unequal participation percent due to the difference of their SoCs and the action of DCC algorithm for modifying the WCC algorithm. Just as the SoCs are converged by the DCC algorithm, the WCC algorithm proportionally shares the power between BESs in accordance with their capacity.

To examine the proposed controller performance when the SoCs of some units violate the allowed limits, the initial SoCs are set according to Fig. 12(a). Other simulation conditions and parameters are kept unchanged. Figure 12(a) shows the SoC variations during the day. Although the initial value of SoC1 is %60, $\varepsilon_1$ is controlled such that SoC1 gets close to other SoCs as much as possible and prevents BES1 from early saturation in charge mode. However, the BES1 violates the maximum allowed limit ($SoC_{max}$), indicated by an arrow in Fig. 12(a). This unit is disconnected from the network under this condition. At this point, $\varepsilon_1 = 0$ and, consequently, $P_{BES,1}^{ref}$ becomes zero according to (28). After a while, a similar event happens to BES2 and BES3, as indicated in Fig. 12(a) where their batteries are fully charged. In comparison with Fig. 11(b), where the initial SoCs have smaller values, the SoC of BESs are closer to $SoC_{max}$ at the end of the charge mode.

Figure 12(b) illustrates the PCF variations of different BESs. At the beginning of the charge mode, the PCFs are determined considering the initial SoCs. For example, if the initial SoC is greater than the system average value (BESs 1-3), then $\varepsilon_n < 1$. Thus, the relevant BES absorbs less power than the value determined by WCC algorithm. Conversely, the unit with a SoC smaller than the system average value (BESs 4-5 and 8-9), has more participation. An $\varepsilon_n = 0$ implies that the SoC of battery has reached to the maximum/minimum allowed limits. Therefore, the BES should be removed from the voltage regulation process.

To demonstrate the operation of distributed control strategy in the case that the droop control and the DCC algorithm are only applied without the WCC algorithm, a simulation was conducted with the initial SoCs shown in Fig. 13(b). The DCC algorithm can not ensure the voltage profiles remain within allowed limits, as shown in Fig. 13(a). The BESs 1-3 are not activated and hence, there is not enough storage capacity for voltage regulation. When the power absorption by some BESs (4-7) decrease due to running full of energy,
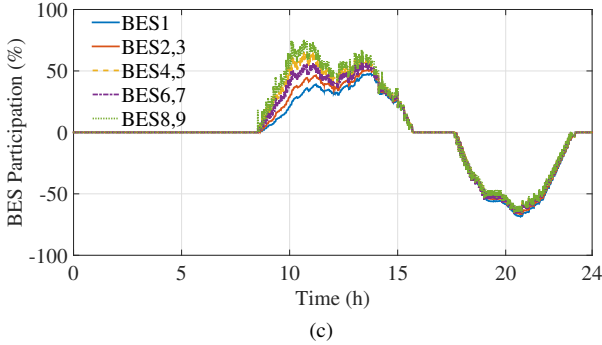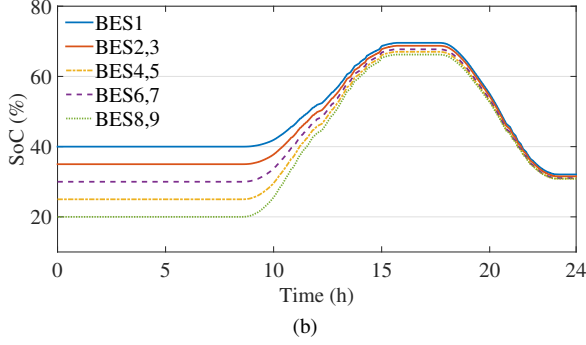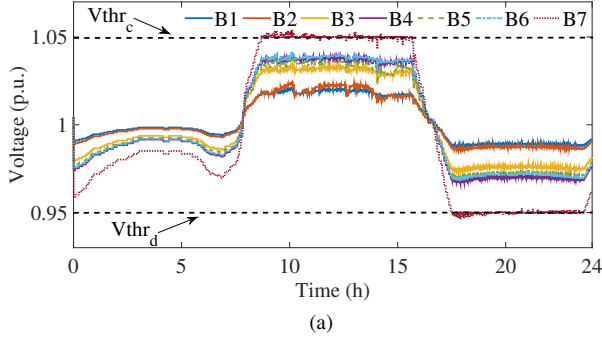
(a)



(b)



(c)

Fig. 11: Coordinated control scheme with DCC algorithm. (a) 24-hour voltage profile; (b) The SoC variations of BESs; (c) BES participation.

the capacity of other BESs (8-9) with lower SoC is less than the required power for voltage control and overvoltage occurs at bus 7. Therefore, the combined control strategy consists of both WCC and DCC algorithms is proposed.

### E. Investigating the Impact of Some Parameters on the Method Performance

The impacts of charging/discharging efficiency and parameter $k$ on the performance of the proposed control method are investigated in this subsection. Figure 14 illustrates the 24-hour SoC variations in case of considering charging/discharging efficiencies according to (29) and (30). As seen, the batteries are charged less than the case of Fig. 11(b), where charging efficiency is assumed 100%, due to the power losses in charge mode. Conversely, the BESs are discharged more than the case of Fig. 11(b) in discharge mode. Although the considered efficiencies affect the charge and discharge values, the
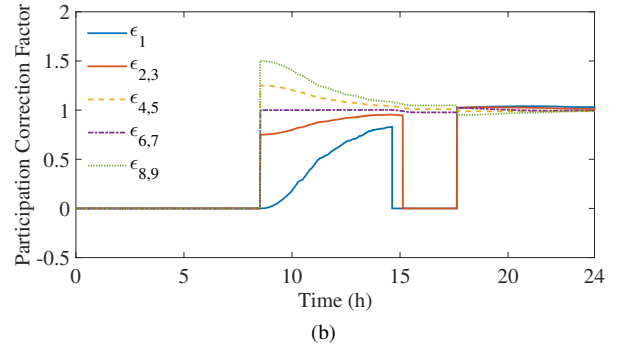
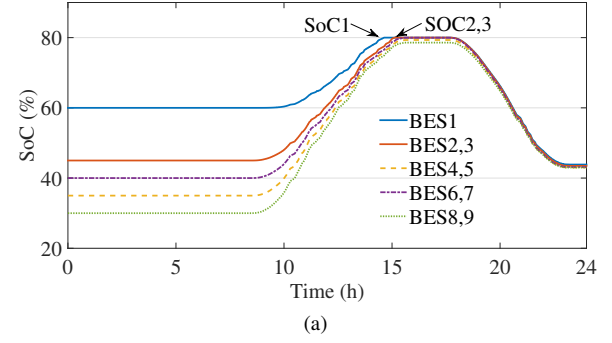

(a)



(b)

Fig. 12: Prevention of SoCs violation from allowed limits. (a) The SoC variations; (b) The PCF variations.
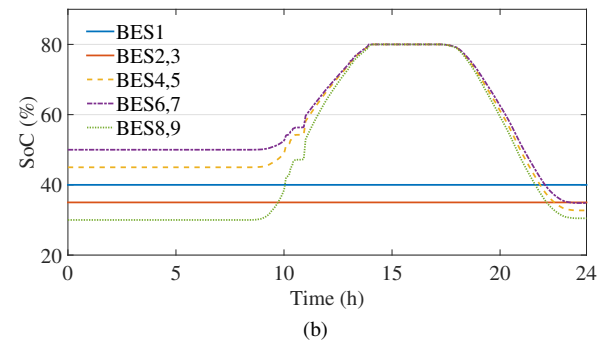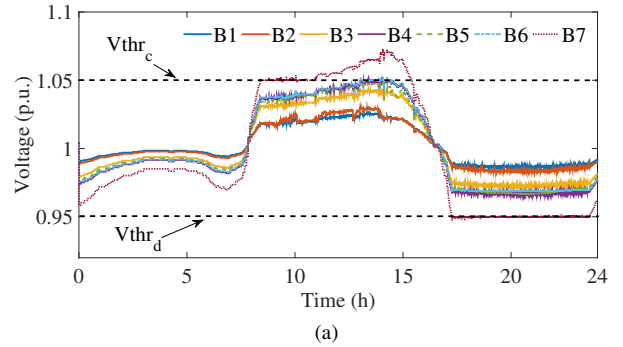


(a)



(b)

Fig. 13: Coordinated control scheme without WCC algorithm. (a) 24-hour voltage profile; (b) The SoC variations.
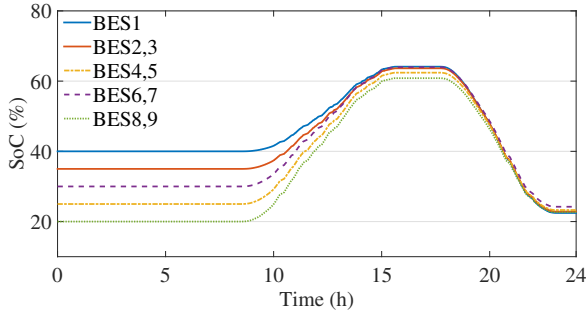
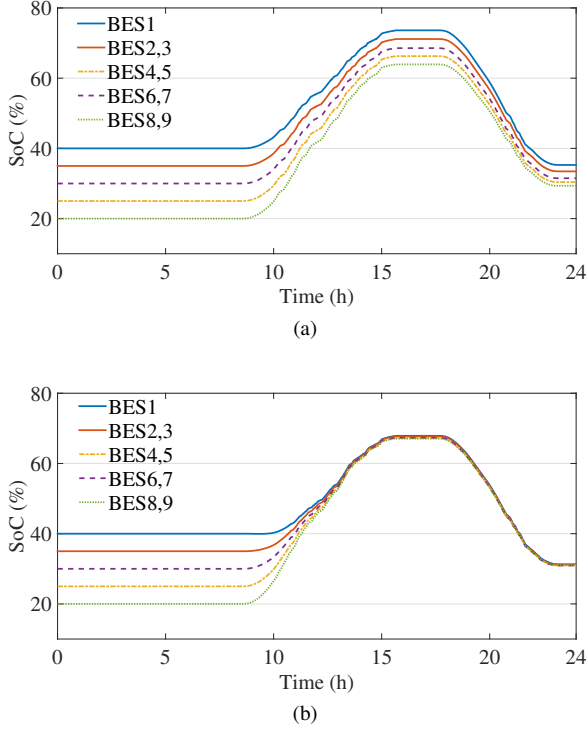Fig. 14: The SoC variations of BESs considering charging/discharging efficiency.



Fig. 15: Convergence speed for different values of parameter $k$. (a) $k$=2; (b) $k$=10.

proposed control scheme present a good performance similar to the previous cases.

The convergence speed dependency of the DCC algorithm on constant $k$ is investigated for different values of $k$ in Fig. 15. It can be ssen that, the larger constant $k$, the faster SoC convergence. The results show that the convergence speed can be adjusted by parameter $k$.

## V. CONCLUSION

In this paper, a new voltage regulation strategy in the low voltage (LV) distribution networks with high PV penetration has been proposed. This method addresses the voltage rise/drop problems using the distributed battery energy storage (BES) systems. Accordingly, a coordinated control scheme has been developed to regulate the system voltage and efficiently utilize the storage capacity of BESs during daily operations. The control scheme contains a local droop based

control method and two consensus algorithms, the weighted consensus control (WCC) and the dynamic consensus control (DCC). The former determines the participation of BESs by regulating their exchanged power in charge/discharge mode based on the installed capacity, while the latter modifies the charging/discharging power calculated in the previous step according to the SoC of batteries in order to keep the BESs' saturation/depletion limitations. The proposed distributed control strategy uses the limited communication links between BESs to implement the algorithms.

The proposed control strategy has been validated by an LV radial distribution feeder that was simulated under different operating conditions in Matlab/Simulink. The test results verified that the control scheme keeps the voltage in the network within the allowed limits during daily operations. Moreover, the power sharing among BESs is automatically established according to the SoC and the installed capacity of batteries.

## REFERENCES

[1] "Renewables 2015 global status report," REN21, Renewable Energy Policy Network for the 21st Century, Tech. Rep., 2015. [Online]. Available: http://www.ren21.net/GSR-2015-Report-Full-report-EN

[2] G. Masson and M. Brunisholz, "IEA PVPS trends 2015 in photovoltaic applications," IEA International Energy Agency, Tech. Rep. IEA-PVPS T1-27:2015, 2015. [Online]. Available: http://www.iea-pvps.org/index.php?id=trends

[3] R. Tonkoski, D. Turcotte, and T. H. M. EL-Fouly, "Impact of high pv penetration on voltage profiles in residential neighborhoods," *IEEE Trans. Sustain. Energy*, vol. 3, no. 3, pp. 518–527, Jul. 2012.

[4] R. A. Shayani and M. A. G. de Oliveira, "Photovoltaic generation penetration limits in radial distribution systems," *IEEE Trans. Power Syst.*, vol. 26, no. 3, pp. 1625–1631, Aug. 2011.

[5] Y. Wang, P. Zhang, W. Li, W. Xiao, and A. Abdollahi, "Online overvoltage prevention control of photovoltaic generators in microgrids," *IEEE Trans. Smart Grid*, vol. 3, no. 4, pp. 2071–2078, Dec. 2012.

[6] F. Olivier, P. Aristidou, D. Ernst, and T. V. Cutsem, "Active management of low-voltage networks for mitigating overvoltages due to photovoltaic units," *IEEE Trans. Smart Grid*, vol. 7, no. 2, pp. 926–936, Mar. 2016.

[7] E. Demirok, P. C. Gonzlez, K. H. B. Frederiksen, D. Sera, P. Rodriguez, and R. Teodorescu, "Local reactive power control methods for overvoltage prevention of distributed solar inverters in low-voltage grids," *IEEE J. Photovolt.*, vol. 1, no. 2, pp. 174–182, Oct. 2011.

[8] S. Hashemi, J. stergaard, and G. Yang, "A scenario-based approach for energy storage capacity determination in lv grids with high pv penetration," *IEEE Trans. Smart Grid*, vol. 5, no. 3, pp. 1514–1522, May 2014.

[9] S. Alyami, Y. Wang, C. Wang, J. Zhao, and B. Zhao, "Adaptive real power capping method for fair overvoltage regulation of distribution networks with high penetration of pv systems," *IEEE Trans. Smart Grid*, vol. 5, no. 6, pp. 2729–2738, Nov. 2014.

[10] S. Weckx, C. Gonzalez, and J. Driesen, "Combined central and local active and reactive power control of pv inverters," *IEEE Trans. Sustain. Energy*, vol. 5, no. 3, pp. 776–784, Jul. 2014.

[11] F. Marra, G. Yang, C. Trholt, J. stergaard, and E. Larsen, "A decentralized storage strategy for residential feeders with photovoltaics," *IEEE Trans. Smart Grid*, vol. 5, no. 2, pp. 974–981, Mar. 2014.

[12] J. von Appen, T. Stetz, M. Braun, and A. Schmiegel, "Local voltage control strategies for pv storage systems in distribution grids," *IEEE Trans. Smart Grid*, vol. 5, no. 2, pp. 1002–1009, Mar. 2014.

[13] M. N. Kabir, Y. Mishra, G. Ledwich, Z. Y. Dong, and K. P. Wong, "Coordinated control of grid-connected photovoltaic reactive power and battery energy storage systems to improve the voltage profile of a residential distribution feeder," *IEEE Trans. Ind. Informat.*, vol. 10, no. 2, pp. 967–977, May 2014.

[14] L. Wang, D. H. Liang, A. F. Crossland, P. C. Taylor, D. Jones, and N. S. Wade, "Coordination of multiple energy storage units in a low-voltage distribution network," *IEEE Trans. Smart Grid*, vol. 6, no. 6, pp. 2906–2918, Nov 2015.

[15] X. Liu, A. Aichhorn, L. Liu, and H. Li, "Coordinated control of distributed energy storage system with tap changer transformers for voltage rise mitigation under high photovoltaic penetration," *IEEE Trans. Smart Grid*, vol. 3, no. 2, pp. 897–906, Jun. 2012.

[16] Y. Wang, K. Tan, X. Peng, and P. So, "Coordinated control of distributed energy storage systems for voltage regulation in distribution networks," *IEEE Trans. Power Del.*, vol. PP, no. 99, pp. 1–1, 2015.

[17] H. Xin, Y. Liu, Z. Qu, and D. Gan, "Distributed control and generation estimation method for integrating high-density photovoltaic systems," *IEEE Trans. Energy Convers.*, vol. 29, no. 4, pp. 988–996, Dec. 2014.

[18] M. J. E. Alam, K. M. Muttaqi, and D. Sutanto, "A novel approach for ramp-rate control of solar pv using energy storage to mitigate output fluctuations caused by cloud passing," *IEEE Trans. on Energy Convers.*, vol. 29, no. 2, pp. 507–518, June 2014.

[19] M. J. E. Alam, K. M. Muttaqi, and D. Sutanto', "Mitigation of rooftop solar pv impacts and evening peak support by managing available capacity of distributed energy storage systems," *IEEE Trans. on Power Syst.*, vol. 28, no. 4, pp. 3874–3884, Nov. 2013.

[20] T. R. Oliveira, W. W. A. G. Silva, and P. F. Donoso-Garcia, "Distributed secondary level control for energy storage management in dc micro-grids," *IEEE Trans. on Smart Grid*, vol. PP, no. 99, pp. 1–11, 2016.

[21] T. Morstyn, B. Hredzak, and V. G. Agelidis, "Distributed cooperative control of microgrid storage," *IEEE Trans. on Power Syst.*, vol. 30, no. 5, pp. 2780–2789, Sept. 2015.

[22] T. Morstyn, B. Hredzak, and V. G. Agelidis', "Cooperative multi-agent control of heterogeneous storage devices distributed in a dc microgrid," *IEEE Trans. on Power Syst.*, vol. 31, no. 4, pp. 2974–2986, July 2016.

[23] T. Morstyn, M. Momayyezan, B. Hredzak, and V. G. Agelidis, "Distributed control for state of charge balancing between the modules of a reconfigurable battery energy storage system," *IEEE Trans. on Power Electronics*, vol. PP, no. 99, pp. 1–1, 2016.

[24] L. Y. Wang, C. Wang, G. Yin, F. Lin, M. P. Polis, C. Zhang, and J. Jiang, "Balanced control strategies for interconnected heterogeneous battery systems," *IEEE Trans. on Sustain. Energy*, vol. 7, no. 1, pp. 189–199, Jan. 2016.

[25] H. Xin, M. Zhang, J. Seuss, Z. Wang, and D. Gan, "A real-time power allocation algorithm and its communication optimization for geographically dispersed energy storage systems," *IEEE Trans. on Power Syst.*, vol. 28, no. 4, pp. 4732–4741, Nov. 2013.

[26] Y. Xu, W. Zhang, G. Hug, S. Kar, and Z. Li, "Cooperative control of distributed energy storage systems in a microgrid," *IEEE Trans. on Smart Grid*, vol. 6, no. 1, pp. 238–248, Jan. 2015.

[27] "IEEE Standard for Interconnecting Distributed Resources with Electric Power Systems," *IEEE Std. 1547-2003*, 2003.

[28] L. Y. Wang, C. Wang, G. Yin, and Y. Wang, "Weighted and constrained consensus for distributed power dispatch of scalable microgrids," *Asian Journal of Control*, vol. 17, no. 5.

[29] D. P. Spanos, R. Olfati-saber, and R. M. Murray, "Dynamic consensus for mobile networks," 2005.

[30] V. Nasirian, S. Moayedi, A. Davoudi, and F. L. Lewis, "Distributed cooperative control of dc microgrids," *IEEE Trans. on Power Electron.*, vol. 30, no. 4, pp. 2288–2303, Apr. 2015.

[31] Q. Shafiee, T. Dragicevic, J. C. Vasquez, and J. M. Guerrero, "Hierarchical control for multiple dc-microgrids clusters," *IEEE Trans. on Energy Convers.*, vol. 29, no. 4, pp. 922–933, Dec. 2014.

[32] H. Cai and G. Hu, "Distributed control scheme for package-level state-of-charge balancing of grid-connected battery energy storage system," *IEEE Trans. on Ind. Inform.*, vol. PP, no. 99, pp. 1–1, 2016.

[33] F. A. Amoroso and G. Cappuccino', "Advantages of efficiency-aware smart charging strategies for {PEVs}," *Energy Conversion and Management*, vol. 54, no. 1, pp. 1 – 6, 2012.

**Mehdi Zeraati** received the B.Sc. and M.Sc. degrees with honors in Electrical Engineering from University of Kashan, Kashan, Iran, in 2010 and 2012, respectively. He is currently pursuing the Ph.D. degree in Electrical Engineering at Isfahan University of Technology, Isfahan, Iran.

His research interests include hierarchical and cooperative control in microgrids, renewable energy resources, distributed control algorithms, and smart grids.

**Mohamad Esmail Hamedani Golshan** was born in Isfahan, Iran, in 1964. He received the B.Sc. degree from the Isfahan University of Technology, Isfahan, Iran, in 1987; the M.Sc. degree from the Sharif University of Technology, Tehran, in 1990; and the Ph.D. degree from the Isfahan University of Technology, Isfahan, Iran, in 1998, all in Electrical Engineering.

He is currently a Professor with the Department of Electrical and Computer Engineering, Isfahan University of Technology. His major research interests are power system analysis, power system dynamics, power quality, dispersed generation, flexible ac transmission systems and custom power, and load modeling special arc furnace modeling.

**Josep M. Guerrero** (S'01–M'04–SM'08–FM'15) received the B.S. degree in telecommunications engineering, the M.S. degree in electronics engineering, and the Ph.D. degree in power electronics from the Technical University of Catalonia, Barcelona, in 1997, 2000 and 2003, respectively. Since 2011, he has been a Full Professor with the Department of Energy Technology, Aalborg University, Denmark, where he is responsible for the Microgrid Research Program. From 2012 he is a guest Professor at the Chinese Academy of Science and the Nanjing University of Aeronautics and Astronautics; from 2014 he is chair Professor in Shandong University; and from 2015 he is a distinguished guest Professor in Hunan University.

His research interests is oriented to different microgrid aspects, including power electronics, distributed energy-storage systems, hierarchical and cooperative control, energy management systems, and optimization of microgrids and islanded minigrids; recently specially focused on maritime microgrids for electrical ships, vessels, ferries and seaports. Prof. Guerrero is an Associate Editor for the IEEE TRANSACTIONS ON POWER ELECTRONICS, the IEEE TRANSACTIONS ON INDUSTRIAL ELECTRONICS, and the IEEE INDUSTRIAL ELECTRONICS MAGAZINE, and an Editor for the IEEE TRANSACTIONS ON SMART GRID and IEEE TRANSACTIONS ON ENERGY CONVERSION. He has been Guest Editor of the IEEE TRANSACTIONS ON POWER ELECTRONICS Special Issues: Power Electronics for Wind Energy Conversion and Power Electronics for Microgrids; the IEEE TRANSACTIONS ON INDUSTRIAL ELECTRONICS Special Sections: Uninterruptible Power Supplies systems, Renewable Energy Systems, Distributed Generation and Microgrids, and Industrial Applications and Implementation Issues of the Kalman Filter; and the IEEE TRANSACTIONS ON SMART GRID Special Issue on Smart DC Distribution Systems. He was the chair of the Renewable Energy Systems Technical Committee of the IEEE Industrial Electronics Society. He received the best paper award of the IEEE TRANSACTIONS ON ENERGY CONVERSION for the period 2014-2015. In 2014 and 2015 he was awarded by Thomson Reuters as Highly Cited Researcher, and in 2015 he was elevated as IEEE Fellow for his contributions on "distributed power systems and microgrids."